Inorganic Chemistry

Article

pubs.acs.org/IC

A Novel PbS Hierarchical Superstructure Guided by the Balance between Thermodynamic and Kinetic Control via a Single-Source Precursor Route

Xiaochuan Duan, Jianmin Ma, Yan Shen, and Wenjun Zheng*

Department of Materials Chemistry, Key Laboratory of Advanced Energy Materials Chemistry (MOE), and TKL of Metal and Molecule-Based Material Chemistry, College of Chemistry, Nankai University, 94 Weijin Road, Tianjin, 300071, People's Republic of China

Supporting Information

ABSTRACT: In this work, a novel lead sulfide (PbS) hierarchical superstructure, denoted as octapodal dendrites with a cubic center, has been synthesized employing a simple single-source precursor route. Our experimental results demonstrate that the novel hierarchical superstructure was generated through the delicate balance between the kinetic growth and thermodynamic growth regimes. Moreover, the morphology of PbS crystals can be controlled by adjusting the solvent under a thermodynamically or kinetically controlled growth regime. It is highly expected that these findings will be useful in understanding the formation of PbS nanocrystals with different morphologies, which are also applicable to other face-centered cubic nanocrystals.

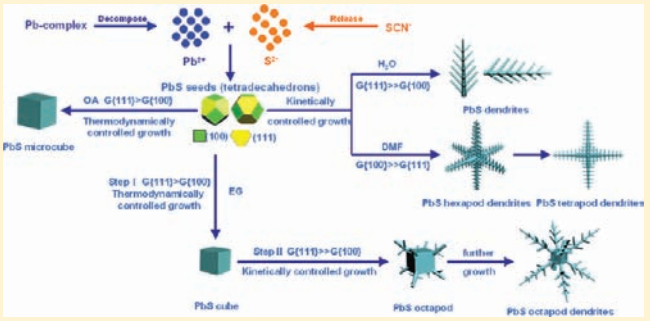

INTRODUCTION

Generally, the growth process of crystals can be separated into two steps, an initial nucleating stage and a subsequent crystal growth process.[1−3] At the initial nucleating stage, the crystalline phase of the seeds is critical for directing the intrinsic shapes of the crystals due to its characteristic symmetry and structure. The preferential nucleation process will occur to make the system energy minimization.[1] At the subsequent growth step, there are several important factors that can greatly influence the final morphology of crystals. These include the intrinsic surface energy of different crystal surfaces, the molecules selectively adsorbed on the surfaces, and the choice of the crystal growth regime, that is, thermodynamic- or kinetic-controllable growth processes.[4] In general, both thermodynamic and kinetic approaches can be employed to control the morphology of a nanocrystal. The thermodynamic control, including the use of a capping agent, is based on the requirement to minimize the total surface energy of a system. It is usually via a slow, nearly layer-by-layer monomer addition onto the crystallite faces to yield stable morphologies.[5,6] In contrast, the kinetic control is based on manipulation of the growth rate at which atoms are generated and added to the surface of a growing seed. Under the kinetic growth regime, anisotropic growth along the kinetically most favorable direction with low activation energy barriers is preferential.[7−9] The crystal growth stage strongly governs the final architecture of the crystals through the delicate balance between the kinetic growth and thermodynamic growth regimes. Take the face-centered cubic (fcc) structure as an example, which has been extensively studied; the thermodynamic control is most successful in generating nanocrystals that are enclosed by a convex surface and low-energy facets, with typical examples including cube, octahedron, tetrahedron, cuboctahedron, decahedron, and icosahedron.[10] Meanwhile, fast nanocrystal growth and formation of branched morphologies have been shown to be characteristic of growth in a kinetically controlled growth regime; notable examples include nanocrystals enclosed by high-energy facets and/or with a concave structure on the surface.[11]

As a rock salt structure, lead sulfide (PbS) has a fcc structure. PbS was chosen in this work due to its prospective applications in solar absorbers, optical switches, photography, and infrared detectors.[12,13] Excellent studies on the synthesis of PbS nanocrystals with tunable size and various shapes have been carried out, and great achievements have been made. Among the numerous methods developed for the shape-controlled synthesis of PbS nanocrystals, the single-source molecular precursor route obviously has some appealing features. The single-source molecular precursors to PbS that have been investigated in those contexts include lead dithiocarbamato complexes,[14] Pb-(DDTC)$_2$,[15] and lead dichalcogenoimidodiphoshanto complexes,[16] [Pb(2-pyc)(NCS)]$_n$.[17] Thermal decomposition of these precursors either in refluxing organic solvent or in the solid state or in metalorganic chemical vapor deposition (MOCVD) can lead to PbS microcrystals or thin films with different morphologies. In this work, we employed the lead hydroxy thiocyanate (Pb(OH)SCN) as the precursor for the first time. Compared with a complex organic precursor, such a simple and cheap inorganic precursor is more environmentally friendly according to the point of "green" chemistry. Specifically, by solvothermal decomposition of the precursor in ethylene glycol (EG) at

Received: August 29, 2011
Published: January 4, 2012

   dx.doi.org/10.1021/ic201889n | *Inorg. Chem.* 2012, 51, 914−919

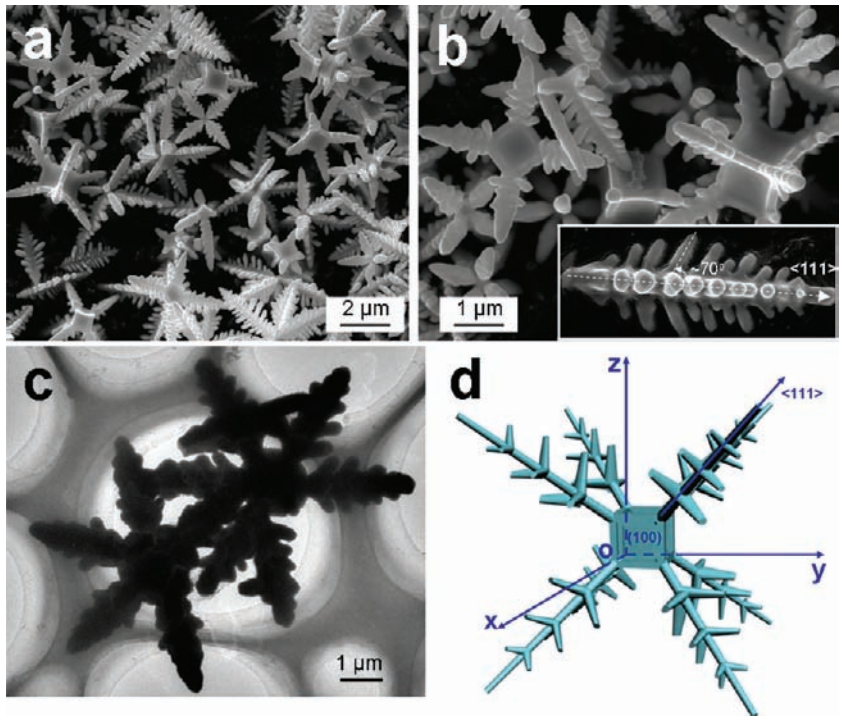

Figure 1. (a) Low- and (b) high-magnification SEM images of PbS octapodal dendrites with a cubic center; (c) TEM images of two typical octapodal dendrites; (d) 3D structural model of octapodal dendrites with a cubic center. The inset in (b) shows a typical SEM image of a single arm fallen from the octapodal dendrites with a cubic center.

200 °C for 12 h, we can obtain a novel PbS hierarchical superstructure, denoted as octapodal dendrites with a cubic center, which have very rarely been reported. Moreover, the morphology of PbS crystals can be controlled by adjusting the solvent under a thermodynamically or kinetically controlled growth regime. It is highly expected that these findings are useful in understanding the formation of PbS nanocrystals with different morphologies, which are also applicable to other fcc nanocrystals.

EXPERIMENTAL SECTION

Synthesis of PbS Microcrystals with Various Morphologies. All reagents were analytical grade and used without any further purification. The single-source molecular precursor (Pb(OH)SCN) was synthesized according to the procedures reported in previous literature reports.[18] It was prepared directly through the precipitation reaction of 5 mmol of lead acetate ($Pb(CH_3COO)_2{\cdot}3H_2O$) and 20 mmol of potassium thiocyanate (KSCN) in 100 mL of distilled water at room temperature in the air for 4 h with vigorous stirring. The as-formed precipitates were filtered, washed with ethanol several times, and dried in vacuum at 60 °C. In a typical process of PbS microcrystals, 0.27 g of the as-prepared Pb(OH)SCN precursor was put into 25 mL of different solvents such as distilled water, ethylene glycol (EG), oleic acid (OA), and *N*,*N*-dimethyl formamide (DMF) was added, respectively. Then, the above solution was transferred into a 30 mL Teflon-lined stainless steel autoclave, sealed, and then heated to 200 °C for 12 h. When the reaction was completed, the autoclave was cooled to room temperature naturally. The resultant product was collected and washed with deionized water and anhydrous ethanol several times until the solution was neutral. The final red product was dried in a vacuum at 80 °C for 3 h.

On-Site Etching Methods. In a typical process of on-site etching text: 0.5 mmol of the as-prepared PbS microcubes (decomposed the precursor in OA) was put into 25 mL of EG under vigorous stirring. Subsequently, 0.1 mmol of lead nitrate ($Pb(NO_3)_2$) and 0.1 mmol of potassium thiocyanate (KSCN) were added into the above solution under continuous stirring. Then a certain amount of ammonium hydroxide (NH_4OH, 25%) was added into the above solution under continuous stirring. After being stirred for 20 min, the total solution was transferred into a stainless-steel autoclave with a capacity of 30 mL, sealed, and heated at 200 °C for 12 h. When the reaction was completed, the autoclave was cooled to room temperature naturally. The resultant product was collected and washed with deionized water and anhydrous ethanol several times until the solution was neutral. The final red product was dried in a vacuum at 80 °C for 3 h. In contrast, we use 0.5 mmol of the as-prepared Pb(OH)SCN precursor instead of $Pb(NO_3)_2$ and KSCN with other experimental conditions unchanged.

Postinstallation Etching Methods. In a typical process of on-site etching text: 0.5 mmol of the as-prepared PbS microcubes (decomposed the precursor in OA) was put into 25 mL of EG under vigorous stirring. Subsequently, a certain amount of ammonium hydroxide (NH_4OH, 25%) was added into the above solution under continuous stirring. After being stirred for 20 min, the total solution was transferred into a stainless-steel autoclave with a capacity of 30 mL, sealed, and heated at 200 °C for 12 h. When the reaction was completed, the autoclave was cooled to room temperature naturally. The resultant product was collected and washed with deionized water and anhydrous ethanol several times until the solution was neutral. The final red product was dried in a vacuum at 80 °C for 3 h.

Characterizations. The products were characterized by X-ray diffraction (XRD), scanning electron microscopy (SEM), transmission electron microscopy (TEM), and high-resolution TEM (HR-TEM) measurements. XRD measurements were performed on a Rigaku D/max 2500 diffractometer with Cu Kα radiation (λ = 0.154056 nm) at V = 40 kV and I = 150 mA, and the scanning speed was 8°/min. Morphology observations were performed on a JEOLJSM-6700F field emission scanning electron microscope (FE-SEM). TEM and HR-TEM images were recorded with a Tecnai G2 20S-Twin transmission electron microscope operating at an accelerating voltage of 120 kV.

RESULTS AND DISCUSSION

The morphologies of the as-synthesized PbS hierarchical superstructures in EG at 200 °C were examined by SEM and TEM, as shown in Figure 1. Figure 1, panels a and b show the

dx.doi.org/10.1021/ic201889n | *Inorg. Chem.* 2012, 51, 914–919

low- and high-magnification SEM images of the structures, respectively. It can be seen that the octapodal dendrites with a cubic center were formed due to accelerated growth along the ⟨111⟩ directions from the corners of a cubic center. Some broken dendrites which have fallen from the cube can be found due to vigorous movement and impingement in a high-temperature and high-pressure environment. The inset in Figure 1b shows a typical SEM image of a single arm fallen from the cubic center. The arm possessed a hierarchical structure with 3-fold symmetry. The angles between these groups of branches and the trunk in the image are typically ~70°, near the theoretical angle 67.8° between two ⟨111⟩ directions of the fcc structure in the {112} projection plane, indicating that the dendrites grow along the ⟨111⟩ direction.[19] The TEM image clearly shows that the cubic centers are in uniform size with an edge length of about 1 μm, and the arms are about 1−3 μm long, which have about 40−60 nm tips and 200−500 nm diameters at the base of the arm. On the basis of the above analyses, we can propose a three-dimensional model as shown in Figure 1d.

It is well-known that for fcc structure, the cube is the thermodynamically stable morphology, while branched morphologies have been shown to be characteristic of growth in a kinetically controlled growth regime. So our result, octapodal dendrites with a cubic center, is highly interesting and to the best of our knowledge the first observation of this hierarchical superstructure guided by a delicate balance between the kinetic growth and thermodynamic growth regimes. To obtain a better understanding of the growth mechanism of the novel hierarchical PbS microcrystals, a time-dependent experiment was carried out at 200 °C for 1, 4, 8, 10, 12 h in EG without any surfactant. XRD patterns of the obtained PbS microcrystals at different stages are similar (Figure 2), which can be easily indexed to the rock salt structure of PbS (JCPDS file No. 05-0592) except for the peak intensities, especially for {111} and {200}. Compared with 0.85, the peak intensity ratio for {111} to {200} given in the JCPDS card, a distinct increase for the ratios occurred (from 0.87 to 1.1), indicating the preferred growth along the ⟨111⟩ directions with a prolonged reaction time.

As reported,[20] Pb^{2+} could react with EG to form a $Pb(eg)_2^{2+}$ organometallic complex, which was stable only at the lower temperatures; however, $Pb(eg)_2^{2+}$ decomposed rapidly upon a temperature increase close to the boiling point (195 °C) of the EG solvent. In the first hour of the reaction temperature increase to 200 °C (Stage I), $Pb(eg)_2^{2+}$ is relatively stable and slowly releases Pb^{2+}, leading to slow nucleation. Low concentrations of PbS nuclei are produced, making the particles grow relatively slowly from nuclei. The driving force for the particle shape under these conditions is the diffusion of adnuclei to form faceted surfaces to minimize the final surface energy of the nuclei. This is a permission of a thermodynamic control process, governed by the habit of a rock salt structure. For fcc structure, a nanocrystal often originates from a tetradecahedral nucleus or seed that is enclosed by six {100} planes and eight {111} planes, and the final shapes are mainly attributed to the differences in the growth rate between the {111} and {100} planes of the tetradecahedral seed.[21] The habit of a rock salt structure reveals that the {111} planes have higher energy than that of the {100} due to a higher packing density and the larger number of under-coordinated atoms. This leads to the formation of PbS microcubes because the {100} plane is the thermodynamically stable plane (Figure 3-a1).

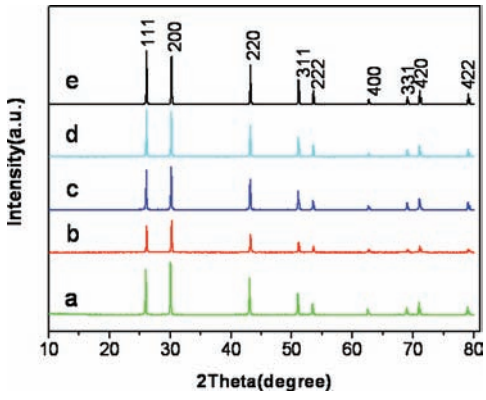

Figure 2. XRD patterns of PbS octapodal dendrites synthesized for (a) 1 h, (b) 4 h, (c) 8 h, (d) 10 h, and (e) 12 h in EG, respectively.

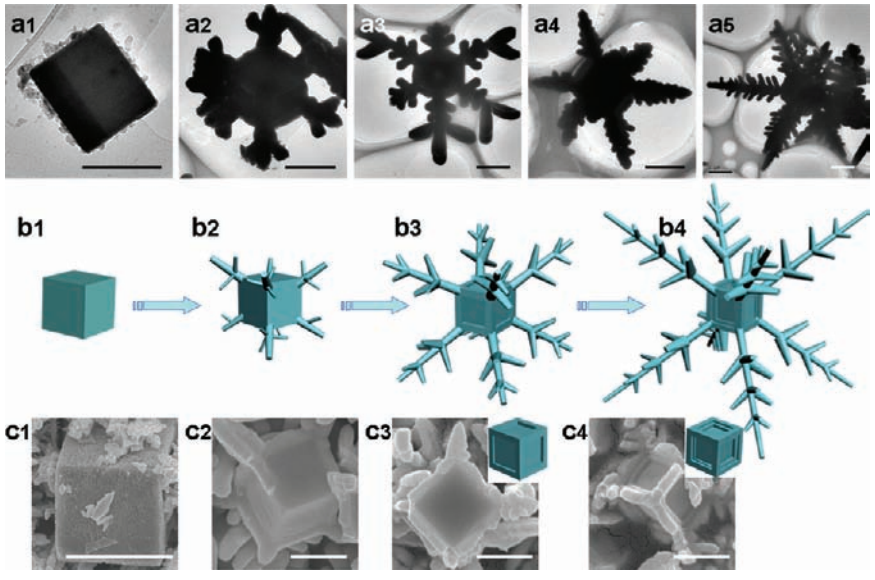

Figure 3. (a) TEM images of PbS octapodal dendrites obtained at different reaction times: 1, 4, 8, 10, and 12 h for columns 1−5, respectively; (b) scheme for the shape evolution of octapodal dendrites with a cubic center; (c) the selective protection and etching process of the cubic surface (inset of c3 and c4 are corresponding 3D structural models). The scale bar is 1 μm.

dx.doi.org/10.1021/ic201889n | Inorg. Chem. 2012, 51, 914−919

When the reaction temperature is maintained at 200 °C (Step II), the $Pb(eg)_2^{2+}$ complexes decompose and release a large number of free Pb^{2+}. At this stage, progressive nucleation would occur in the presence of large amounts of Pb^{2+}; such high supersaturation can easily result in high-speed growth of PbS nuclei. Such post growth would shift the growth mode to the kinetic growth regime. According to the Berg effect, the concentration of reaction ions over the surface is not uniform, which is supposed to decrease in the order of corner, edge, and side face.[22] The overgrowth can be facilitated at corners due to a large number of dangling bonds. The {111} and {100} planes in the PbS crystal lattice are different in the surface atom structures (Figure S1, Supporting Information) and bonding as well as the possibility of chemical reactions. The adsorption and deadsorption of the PbS seeds on the different planes may kinetically favor the preferential crystal growth along eight ⟨111⟩ directions (G{111} ≫ G{100}, G{111} represents the growth rate of the {111} planes). A significant change in the morphology is gradually taking place; a cubic center has eight short arms growing along the ⟨111⟩ directions from the eight corners of a cubic core with {100} terminating (Figure 3-a2). Then the arms grow up along the ⟨111⟩ directions with prolonged reaction time (the growth model can be seen in Figure 3b). Compared with the previously reported PbS hierarchical dendrites, the central cube of the octapodal dendrites is integrally preserved, while others reported in the previous literature reports only serve as unstable intermediates and are not retained in the final morphology.[23−30] Besides the rapid change between the two different growth models, the OH^- ions (from the precursor) play an important role in protecting the cubic center by selectively passivating the {100} planes, which is consistent with the previous reports.[31,32] The chemisorption of OH^- ions on the {100} planes also greatly blocks the addition of PbS nuclei to the {100} planes of a growing seed, which may greatly strengthen the Berg effect and facilitate overgrowth at corners of the cubic center. As such, the PbS nuclei at corners could stay to grow along the ⟨111⟩ directions to form the final octapodal dendrites. The etching effect of OH^- ions on the {100} planes can be clearly seen in Figure 3c, indicating the strong chemical interaction between OH^- ions and the {100} planes of the PbS cubic center.

On the basis of the above analysis, the morphology of PbS crystals can be controlled by adjusting the solvent in line with forming different Pb-complexes, leading to the different release temperatures (boiling point of the solvent) and release rates of Pb^{2+} ions. We use the same precursor, and reaction conditions

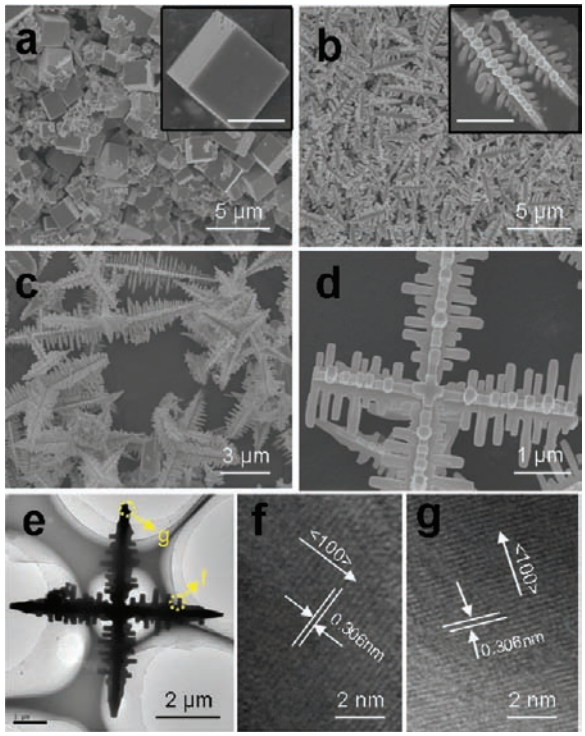

Figure 4. Low magnification SEM images of the as-synthesized PbS samples in different solvents: (a) OA, (b) distilled water, (c, d) DMF (inset of a and b are corresponding high magnification images and show the typical PbS microcube and dendrites; the scale bar is 2 μm); (e) TEM image and (f, g) corresponding HRTEM images of tetrapodal dendrites.

Scheme 1. Schematic Illustration of the Formations of PbS Microcrystals with Various Morphologies in Different Solvents under Thermodynamically or Kinetically Controlled Growth Regime[a]

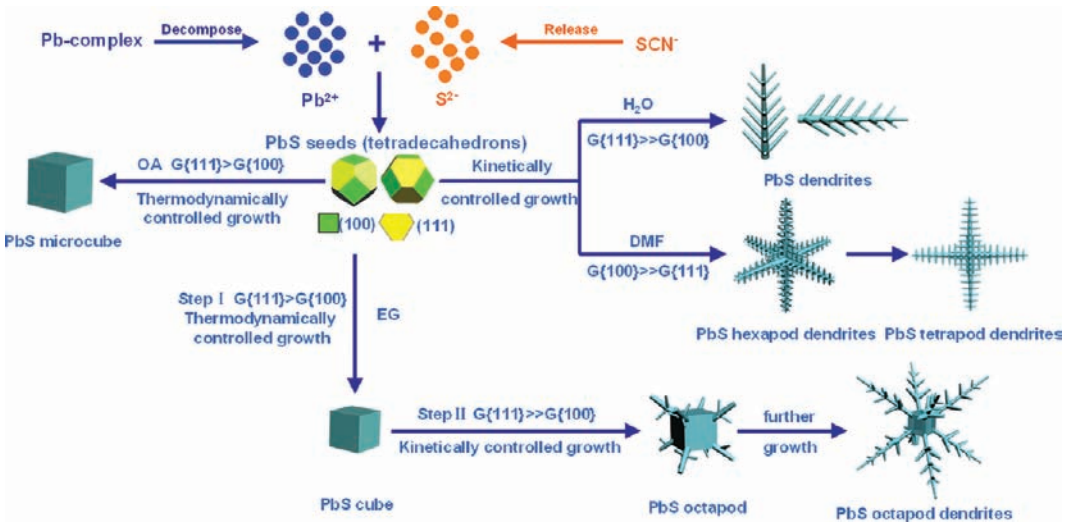

[a]All the microcrystals were formed originally from the tetradecahedral seeds. The formation of different morphologies were mainly attributed to the differences in the growth rate between the {111} and {100} planes of the seed.

dx.doi.org/10.1021/ic201889n | Inorg. Chem. 2012, 51, 914−919

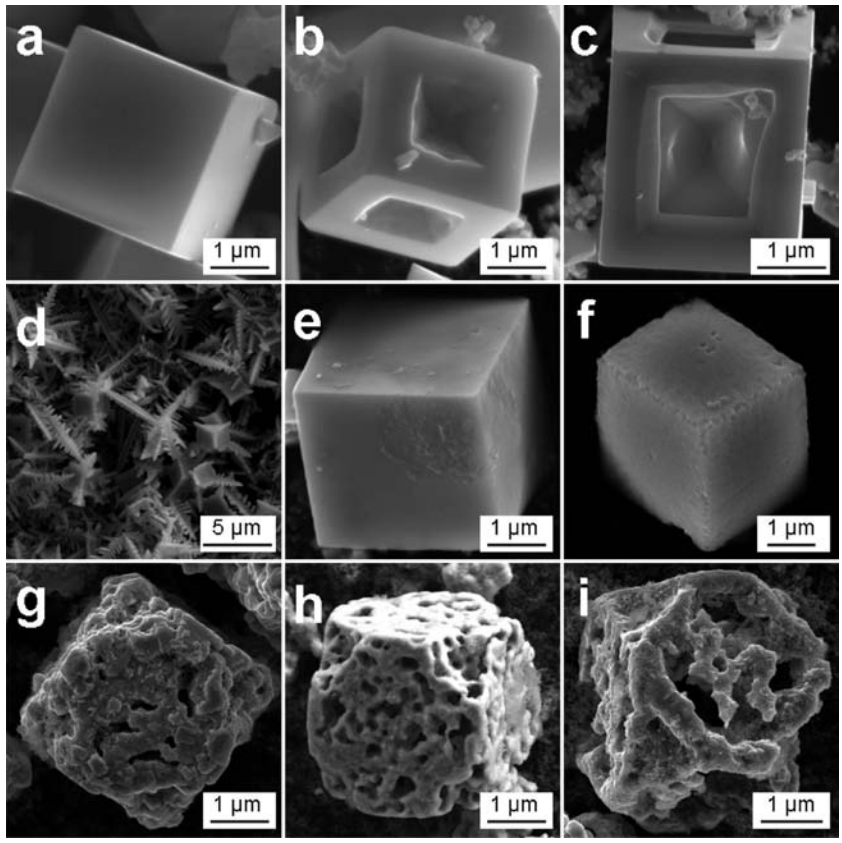

Figure 5. SEM images of the PbS microcubes in different etching process, on-site etching process in the presence of lead nitrate and potassium thiocyanate with different amounts of ammonium hydroxide: (a) 0.5 mL; (b) 1 mL; (c) 2 mL. (d) Using the as-prepared Pb(OH)SCN precursor as the source with 1 mL of ammonium hydroxide. Postinstallation etching process in the absence of a lead source and sulfur source with different amounts of ammonium hydroxide: (e) 0.5 mL; (f) 1 mL; (g) 1.5 mL; (h) 2 mL; (i) 2.5 mL.

(temperature and time) are kept the same for all of the reactions (XRD patterns of the as-synthesized samples in different solvents can be seen in Figure S2, Supporting Information); the only significant difference is the solvent used: oleic acid (OA, boiling point is 285 °C), distilled water (boiling point is 100 °C), and *N*,*N*-dimethyl formamide (DMF, boiling point is 153 °C). Because of the high boiling point, a slow decomposition of $Pb(OA)_2^{2+}$ will occur when OA was used as the solvent. Slow crystal growth suggests that the shape of PbS is generated mainly under a thermodynamically preferential crystal growth regime, leading to the formation of cubic morphology (the most thermodynamically stable; see Figure 4a). Because the decomposition temperatures are lower than the reaction temperature (200 °C) in distilled water and DMF, progressive nucleation would occur at the beginning of growth. In this case, the growth is driven by a kinetically controlled trend, resulting in the formation of dendritical morphology (Figure 4). Specifically, unlike in EG and distilled water ($G\{111\} \gg G\{100\}$), the selectively chemisorption of DMF molecules on {111} planes can impede the addition of PbS nuclei to the {111} planes in the growth process, causing G{111} to be much less than G{100}.[33,34] So the dendrites grow along six ⟨100⟩ directions to form hexapodal dendrites. Because of the vigorous movement and impingement under hydrothermal condition, the tetrapodal dendrites can also be observed. It is reasonably believed that the tetrapodal dendrites may originate from the broken hexapodal dendrites. Overall, our proposed reaction mechanism in Scheme 1 is able to explain successfully the formation of octapodal dendrites with a cubic center in EG and other morphologies in different solvents.

It is worth noting that the OH^- ions play different roles at different stages of the PbS octapodal dendrites growth process. Specifically, the OH^- ions protect the cubic center by selectively passivating the {100} planes at the early stages of crystal growth. With depletion of the starting species, another important role of the OH^- ions, etching takes place during the later stages of crystal growth owing to the slow growth rate. To understand the two opposing factors of OH^- ions, two controllable experiments were further carried out. The first experiment was carried out in the presence of a small amount of lead nitrate and potassium thiocyanate (0.1 mmol), which is called the on-site etching process. By adjusting the amount of ammonium hydroxide, PbS microcubes with different degree etching {100} planes can be obtained (Figure 5a–c). Adding a small amount of lead source and sulfur source can promote the dissolution–reprecipitation process. So the etching gradually occurs by the surface to the center of {100} planes. When using the as-prepared Pb(OH)SCN precursor as the source, we can also obtain PbS octapodal dendrites with a cubic center (Figure 5d). The other experiment was carried out without adding a lead source and sulfur source, which is called the postinstallation etching process. Unlike the on-site etching process, the fast dissolution rate makes the etching {100} planes irregular (Figure 5e–g). Moreover, with the increase in the amount of ammonium hydroxide, not only the surfaces but also the corners can be etched by OH^- ions (Figure 5h,i).

dx.doi.org/10.1021/ic201889n | *Inorg. Chem.* 2012, 51, 914–919

CONCLUSION

In summary, we reported a novel PbS hierarchical superstructure by solvothermal decomposition of the precursor in EG. The feasible growth mechanism was proposed on the basis of the characterizations, indicating that the octapodal dendrites with a cubic center were guided by a delicate balance between the kinetic growth and thermodynamic growth regimes. As a continuation, we can obtain different morphologies of PbS under thermodynamic or kinetic control by changing the solvent. It is highly expected that our facile synthetic strategy may provide a way to explore the formation of the PbS microcrystals with different morphologies.

ASSOCIATED CONTENT

Supporting Information

The {111} and {100} planes of the PbS crystal and XRD patterns of PbS microcrystals in different solvents. This material is available free of charge via the Internet at http://pubs.acs.org.

AUTHOR INFORMATION

Corresponding Author

*E-mail: zhwj@nankai.edu.cn.

ACKNOWLEDGMENTS

This work was supported by the National Natural of Science Foundation of China (Grant No. 20971070 and 21073095) and MOE (IRT-0927) and the Project Fundamental and Applied Research of Tianjin.

REFERENCES

(1) Buckley, H. E. *Crystal Growth*; Wiley: New York, 1951.
(2) Mann, S. *Angew. Chem.* **2000**, *112*, 3532−3548.
(3) Siegfried, M. J.; Choi, K. S. *Angew. Chem.* **2005**, *117*, 3282−3287.
(4) Tao, A.; Habas, S.; Yang, P. D. *Small* **2008**, *4*, 310−325.
(5) Sun, Y.; Xia, Y. *Science* **2002**, *298*, 2176−2179.
(6) Chou, S. W.; Zhu, C. L.; Neeleshwar, S.; Chen, C. L.; Chen, Y. Y.; Chen, C. C. *Chem. Mater.* **2009**, *21*, 4955−4961.
(7) Zhang, H.; Li, W.; Jin, M.; Zeng, J.; Yu, T.; Yang, D.; Xia, Y. *Nano Lett.* **2011**, *11*, 898−903.
(8) Cheong, S.; Watt, J.; Ingham, B.; Toney, M. F.; Tilley, R. D. *J. Am. Chem. Soc.* **2009**, *131*, 14590−14595.
(9) Ren, J.; Tilley, R. D. *J. Am. Chem. Soc.* **2007**, *129*, 3287−3291.
(10) Lim, B.; Jiang, M.; Tao, J.; Camargo, P.; Zhu, Y.; Xia, Y. *Adv. Funct. Mater.* **2009**, *19*, 189−200.
(11) Ma, Y.; Kuang, Q.; Jiang, Z.; Xie, Z.; Huang, R.; Zheng, L. *Angew. Chem., Int. Ed.* **2008**, *47*, 8901−8904.
(12) Wang, N.; Cao, X.; Guo, L.; Yang, S. H.; Wu, Z. Y. *ACS Nano* **2008**, *2*, 184−190.
(13) Peng, Z.; Jiang, Y.; Song, Y.; Wang, C.; Zhang, H. *Chem. Mater.* **2008**, *20*, 3153−3162.
(14) Trindade, T.; O'brien, P.; Zhang, X. M.; Motevallic, M. *J. Mater. Chem.* **1997**, *7*, 1011−1016.
(15) Lee, S. M.; Jun, Y. W.; Cho, S. N.; Cheon, J. *J. Am. Chem. Soc.* **2002**, *124*, 11244−11245.
(16) Afzaal, M.; Ellwood, K.; Pickett, N. L.; O'Brien, P.; Raftery, J.; Waters, J. *J. Mater. Chem.* **2004**, *14*, 1310−1315.
(17) Aslania, A.; Morsalia, A.; Zeller, M. *Solid State Sci.* **2008**, *10*, 1591−1597.
(18) Lambou, M. G.; Dollear, F. G. *J. Am. Oil. Chem. Soc.* **1946**, *Apr*, 97−100.
(19) Lin, T. H.; Lin, C. W.; Liu, H. H.; Sheu, J. T.; Hung, W. H. *Chem. Commun.* **2011**, *47*, 2044−2046.
(20) Bashouti, M.; Lifshitz, E. *Inorg. Chem.* **2008**, *47*, 678−682.
(21) Jun, Y.; Lee, J. H.; Choi, J.; Cheon, J. *J. Phys. Chem. B* **2005**, *109*, 14795−14806.
(22) Berg, W. F. *Proc. R. Soc. London A* **1938**, *164*, 79−95.
(23) Hong, J. W.; Lee, Y. W.; Kim, M. S.; Kang, W.; Han, S. W. *Chem. Commun.* **2011**, *47*, 2553−2555.
(24) Wang, X.; Xi, G.; Liu, Y.; Qian, Y. *Cryst. Growth Des.* **2008**, *8*, 1406−1411.
(25) Zhu, J. P.; Yu, S. H.; He, Z. B.; Jiang, J.; Chen, K.; Zhou, X. Y. *Chem. Commun.* **2005**, 5802−5804.
(26) Zhang, G.; Lu, X.; Wang, W.; Li, X. *Chem. Mater.* **2007**, *19*, 5207−5209.
(27) Ni, Y. H.; Liu, H. J.; Wang, F.; Liang, Y.; Hong, J. M.; Ma, X.; Xu, Z. *Cryst. Growth Des.* **2004**, *4*, 759−764.
(28) Xiong, S.; Xi, B.; Xu, D.; Wang, C.; Feng, X.; Zhou, H.; Qian, Y. *J. Phys. Chem. C* **2007**, *111*, 16761−16767.
(29) Zuo, F.; Yan, S.; Zhang, B.; Zhao, Y.; Xie, Y. *J. Phys. Chem. C* **2008**, *112*, 2831−2835.
(30) Liu, S.; Xiong, S.; Bao, K.; Cao, J.; Qian, Y. *J. Phys. Chem. C* **2009**, *113*, 13002−13007.
(31) Zhu, T. J.; Chen, X.; Cao, Y. Q.; Zhao, X. B. *J. Phys. Chem. C* **2009**, *113*, 8085−8091.
(32) Zhang, S.; Wu, C.; Wu, Z.; Yu, K.; Wei, J.; Xie., Y. *Cryst. Growth Des.* **2008**, *8*, 2933−2937.
(33) Carbó-Argibay, E.; Rodríguez-González, B.; Pacifico, J.; Pastoriza-Santos, I.; Pérez-Juste, J.; Liz-Marzán, L. M. *Angew. Chem.* **2007**, *119*, 9141−9145.
(34) Tsuji, M.; Maeda, Y.; Hikino, S.; Kumagae, H.; Matsunaga, M.; Tang, X. L.; Matsuo, R.; Ogino, M.; Jiang, P. *Cryst. Growth Des.* **2009**, *9*, 4700−4705.